

# ULTRAVIOLET ASTRONOMY IN THE XXI CENTURY



**e-Workshop 2020 – October 27-29**

# ON THE CREATION OF A STANDARD PHOTOMETRIC SYSTEM FOR ULTRAVIOLET ASTRONOMY

## PROPOSAL FROM THE WORKING GROUP ON ULTRAVIOLET ASTRONOMY DIVISION B (FACILITIES, TECHNOLOGIES AND DATA SCIENCE) INTERNATIONAL ASTRONOMICAL UNION

### Authors:

Ana I Gómez de Castro, Noah Brosch, Daniela Bettoni, Leire Beitia-Antero, Paul Scowen, David Valls-Gabaud, Mikhail Sachkov

### Motivation:

Ultraviolet (UV) astronomy was born in the late 1960's with the advent of space astronomy. Though UV observatories have been scarce, photometric standards are well defined and have been carried over from mission to mission. This scenario is going to change during the next decade with the advent of widely spread cubesat technology. Access to UV data is fundamental in many areas of astrophysical research, however no UV observatories are included in the planning of the main space agencies with the only exception being the Spectrum-UV (WSO-UV) observatory from the Russian space science program. As a result, it is expected that plenty of small, cubesat type missions will be flown to run well defined experiments, including survey type probes.

In this context, it is necessary to define some common grounds to facilitate comparing and contrasting data from different UV missions. The charter of the "UV astronomy working group" (UVA WG) for the period 2018-2020 is to set the grounds for the definition of a UV photometric system suitable to be implemented in small missions and that grows on the scientific challenges addressed by using UV astronomical observations.

The goal of this document is to advocate the community to adopt standards that will allow easy data fusion from different missions.

Document	Circulated to	Date	Final Approval Date
Draft	Members of the UV Astronomy WG	Jan 2020	
Document	IAU Division B, Steering Committee	Jul 2020	
Revised Document	IAU Executive Committee	Dec 2020	
Final Document	General Assembly	July 2021	

## 1. Introduction: UV photometry from already flown missions

The history of UV astronomy is long and begins in 1968 with the launch of the *Orbiting Astronomical Observatory* (OAO-2) that provided the first full survey of the UV sky. The UV range goes from the ozone cut-off, traditionally taken at 320 nm to the X-ray limit (10 nm). The UV range is divided<sup>a</sup> into the near UV or NUV (320-200 nm), the far UV or FUV (200-90 nm) and the extreme UV or EUV (90-10 nm). This proposal only deals with the NUV and FUV ranges.

Given its wavelength coverage, UV astronomy is a native space astronomy. Through the years, several missions have operated in this range being the last ones: the International Ultraviolet Explorer (IUE), 1978-1996, for UV spectroscopy in the 115-315 nm range, the Far UV Spectroscopic Explorer (FUSE), 1999-2007, for spectroscopy in the 90.5-119.5 nm range, the GALaxy Evolution eXplorer (GALEX), 2003-2012, for imaging and slit-less spectroscopy in the 135-280 nm range and the Hubble Space Telescope (HST), launched in 1990 and still operational, to observe in the 100-320 nm range both in imaging and spectroscopic modes.

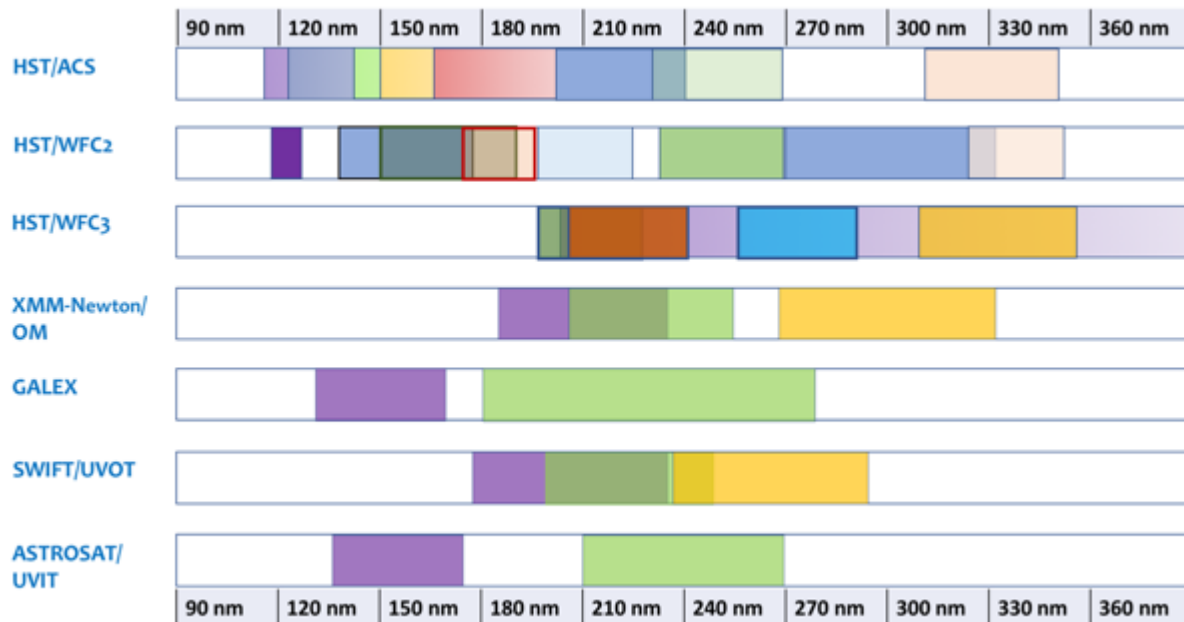


Figure 1. Sketch outlining the spectral coverage of the UV filters (or bands) used for imaging purposes in astronomy (GALEX, HST/ACS, HST/STIS, XMM-Newton/OM, SWIFT/UVOT). Note that the final transmittance also depends on the response of the detector. This is particularly relevant for the MCP type detectors often used in UV Astronomy since they use photocathodes only sensitive to specific spectral ranges. We refer the reader to the Instruments manuals and handbooks for more details on the filters (precise transmittance curves, effective wavelengths etc...); note that, for instance, several ACS filters are step filters that cannot be adequately represented in this plot. Also, filters are many and overlap high in the HST instruments.

Also, SWIFT/UVOT, XMM-Newton/OM and ASTROSAT/UVIT have UV photometric capabilities. In Figure 1, a sketch outlining the UV photometric bands (or filters) used by these missions for

<sup>a</sup> McGraw-Hill Access Science, <https://www.accessscience.com/content/719600>

imaging purposes are displayed; full details can be found in the instruments handbooks made available by the respective missions. The degree of sky coverage is indicated in Table 1 and also displayed in Figure 2 for some representative surveys. Complete graphical information on the sky coverage of the observations made with all instruments and bands in Table 1 can be found in Appendix B.

The band selection at UV wavelengths is mainly determined by sensitivity considerations and by the technological difficulties to build efficient filters and detectors. GALEX was designed as an UV sky surveyor and, as such, the bands were made as broad as possible<sup>b</sup>. The Advanced Camera System (ACS) on HST makes use of many filters that, in the 115-175 nm range, enabled broad band (bandwidth 30-50 nm) imaging by the combination of the transmittance of step filters and the spectral sensitivity of the detector; it is however affected by red-leak problems.

Table 1: UV fields observed before May 2020

FILTER	CENTRAL WAVELENGTH (nm)	Width (nm)	No. of fields	Sky coverage (square deg)	Mean exp. (s)	Median exp. (s)	Total exposure time (s)
<b>HUBBLE SPACE TELESCOPE/ADVANCED CAMERA SYSTEM (HST/ACS), SOLAR BLIND CHANNEL</b>							
F115LP	MgF <sub>2</sub> , 115 nm longpass	N/A	427	5.73	133	100	386,445
F122M	$\lambda_c=142.0$ nm	10	57	0.81	385	201	146,532
F125LP	CaF <sub>2</sub> , 125 nm longpass	N/A	455	6.11	208	100	638,751
F140LP	BaF <sub>2</sub> , 140 nm longpass	N/A	436	2.41	475	440	987,657
F150LP	Quartz, 150 nm longpass	N/A	553	7.43	579	640	1,760,171
F165LP	Fused Silica, 165 nm longpass	N/A	236	7.38	425	375	365,501
<b>HUBBLE SPACE TELESCOPE/ADVANCED CAMERA SYSTEM (HST/ACS), HIGH RESOLUTION CAMERA</b>							
F220W	222.8 nm	48.5	536	0.29	511	356	1,210,901
F250W	269.6 nm	54.9	608	5.55	532	404	1,646,224
F330W	335.4 nm	58.8	554	6.24	292	100	818,912

<sup>b</sup> An important consideration was also that the FUV-NUV color was reddening-free for the average Galactic Extinction Curve.

Table 1: UV fields observed (cont.)

FILTER	CENTRAL WAVELENGTH (nm)	Width (nm)	No. of fields	Sky coverage (square deg)	Mean exp. (s)	Median exp. (s)	Total exposure time (s)
<b>HUBBLE SPACE TELESCOPE/WIDE FIELD PLANETARY CAMERA 2 (HST/WFPC2)</b>							
F160BW	149.2 nm	50.0	313	19.5	673	400	458,943
F170BW	166.6 nm	43.4	222	3.17	590	600	380,502
F185W	189.9 nm	29.7	25	0.35	524	300	51,441
F255W	254.5 nm	40.8	552	7.89	450	300	559,949
F300W	289.2 nm	72.8	3635	52.0	746	700	91,36,280
F336W/ Stromgr. u	331.7 nm	37.1	3065	202.9	529	400	5,493,150
<b>HUBBLE SPACE TELESCOPE/WIDE FIELD CAMERA 3 (HST/WFC3)</b>							
F200LP	488.3 nm <sup>c</sup>	50.2	393	20.42	308	151	356,652
F218W	222.4 nm	32.2	402	5.74	247	25	599,888
F225W	235.9 nm	46.7	586	19.43	350	241	919,340
F275W	270.4 nm	39.8	1998	8.96	506	350	4,248,733
<b>XMM-NEWTON/OPTICAL MONITOR (XMM/OM)</b>							
UVW2	212 nm	50	2228	10.52	2668	2499	44,055,184
UVM2	231 nm	48	4074	19.23	2980	3000	70,732,649
UVW1	291 nm	83	5251	24.79	2730	2500	95,506,682
<b>GALEX</b>							
FUV	152.8 nm	44.2	34199	33264	631	185	21,710,348
NUV	227.1 nm	106.0	44475	39623	898	207	40,230,387
<b>SWIFT/ULTRAVIOLET OPTICAL TELESCOPE (SWIT/UVOT)</b>							
UVW2	203 nm	68.7	41821	3357	1091	536	54,051,180
UVM2	223.1 nm	49.8	46386	3723	1033	529	54,663,428

<sup>c</sup> “Pivot wavelength” is a measure of the effective wavelength of a filter (see [WFC3 Instrument Handbook](#) and Tokunaga & Vacca 2005, *PASP*, **117**, 421). It is calculated here based on the integrated system throughput. Filter transmissions were measured in air, but the equivalent vacuum wavelengths are reported in this table.

UVW1	263.4 nm	69.3	47817	3838	844	299	48,425,796
------	----------	------	-------	------	-----	-----	------------

Table 1: UV fields observed (cont.)

FILTER	CENTRAL WAVELENGTH (nm)	Width (nm)	No. of fields	Sky coverage (square deg)	Mean exposure (s)	Median exposure (s)	Total exposure time (s)
<b>ASTROSAT/ULTRAVIOLET IMAGING TELESCOPE (ASTROSAT/UVIT)</b>							
FUV_F148W	148 nm		689	117.8	7282	5000	366,3114
FUV_F148Wa	148 nm		689	117.8	2999	2500	92,983
FUV_F154W	154 nm		689	117.8	9513	4074	3,967,070
FUV_F169M	169 nm		689	117.8	4821	2800	1,557,452
FUV_F172M	172 nm		689	117.8	5047	2950	1,499,093
NUV_N219M	219 nm		689	117.8	7022	3496	891,816
NUV_N242W	242 nm		689	117.8	7326	3000	923,104
NUV_N245M	245 nm		689	117.8	5456	2978	987,560
NUV_N263M	263 nm		689	117.8	4255	2100	668,119
NUV_N279N	279 nm		689	117.8	5493	3363	901,015

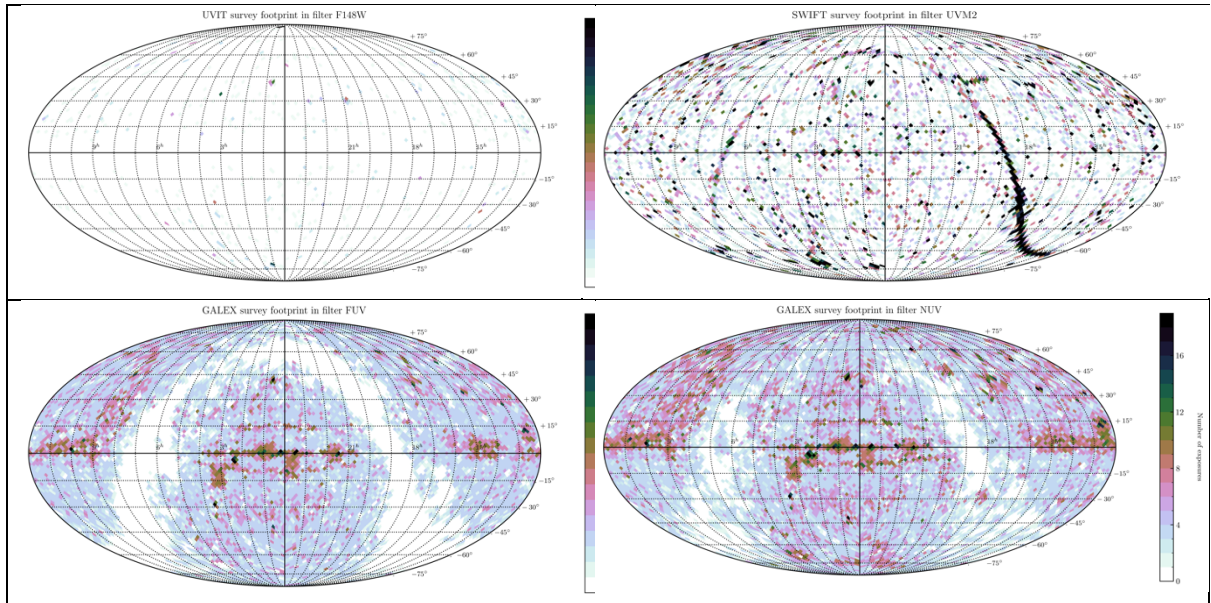


Figure 2. Sky coverage of the observations made with ASTROSAT/UVIT/FUV\_F148W, SWIFT/UVOT/UVM2, GALEX/FUV and GALEX NUV. The total number of exposures in a given region is color coded.

In summary:

The already flown UV missions have implemented instruments for imaging only above 115 nm, the cut-off limit of the MgF<sub>2</sub> used for mirrors coating and also as the material of the sealing window of the MCP detectors operating at wavelengths below 170 nm.

The most often implemented bands are a FUV band (about 140-180 nm) and a NUV band (about 190-250 nm) plus the u-band from the Strömgren photometric system to make the connection with the optical range.

## 2. Spectrophotometric Standards

The UV photometric system is based on the fluxes measured by the TD1 satellite (Thompson et al. 1978); magnitudes and standard errors are derived from absolute fluxes by means of the calibration by Hayes & Latham (1975). Fluxes were measured in the following four bands:

- Central wavelength: 156.5 nm (effective width 33 nm)
- Central wavelength: 196.5 nm (effective width 33 nm)
- Central wavelength: 236.5 nm (effective width 33 nm)
- Central wavelength: 274.0 nm (effective width 31 nm)

none reaches below 140 nm.

The original spectrophotometric standards were defined by the International Ultraviolet Explorer (IUE). They were incorporated later into HST (Bohlin et al. 1990); the 23 original calibration stars and their finding charts can be found in Turnshek et al. (1990). **Currently, there is a set of flux standards in the HST system that constitute the baseline for UV photometry and flux calibration.** The standards can be accessed through [CALSPEC<sup>d</sup>](https://www.stsci.edu/hst/instrumentation/reference-data-for-calibration-and-tools/astronomical-catalogs/calspec) and their main characteristics are summarized in Appendix A (Bohlin et al. 2014). The conversion of the IUE spectra on the white dwarf primary spectrophotometric scale (Bohlin et al. 1995) is described by Bohlin (1994, 1996).

## 3. Foreseen characteristics of the UV filters in small and cubesat size mission

The main constraints for the design of UV filters are:

- The quantum efficiency of the photosensitive substrates used in MCP detectors. As shown in Figures 3a,b detectors sensitive in the far UV are often based on photocathodes that are blind to longer wavelengths, which is a desired feature for many astrophysical applications. However, not all detectors are solar blind; the MAMA detectors on HST instruments or the new generation CCD detectors implemented in

---

<sup>d</sup> Space Telescope Institute

<https://www.stsci.edu/hst/instrumentation/reference-data-for-calibration-and-tools/astronomical-catalogs/calspec>

WSO-UV spectrographs and imager (Shugarov et al. 2014) are sensitive over the full range.

- The optical properties of materials results in the transmittance of filters to decrease with bandwidth. This effect is especially noticeable at UV wavelengths. The transmittance of a 3-10 nm width filter in the 115-175 nm range barely exceeds 7-10%.
- The 90-120 nm band requires a different observation/detection technology hence, bands such as 110-140nm crossing the 115nm frontier are not easy to implement and, in particular, for cubesat based photometric studies.

Moreover, the definition of the photometric system is conditioned by the environmental conditions in low Earth orbit (e.g. avoiding the main geocoronal lines, especially Lyman-alpha, but also O I and C I).

From the astronomical point of view, there are two important considerations to be made:

- The density of spectral lines increases rapidly with photon energy. However, any definition of the system based on binning the UV range into 3-5 energy bins does not reproduce well the near UV continuum and prevents bands definition for the study of the UV extinction bump.
- The UV bump is produced by the interstellar medium and significantly affects color-based studies of the Galaxy. However, it depends on the line of sight and needs to be quantified for photometric studies prior to populations analysis.

Additional desirable features are:

1. The GALEX FUV and NUV bands should be easily integrated in the system
2. An extension to the atmospheric cut-off reaching 350nm is highly desirable.

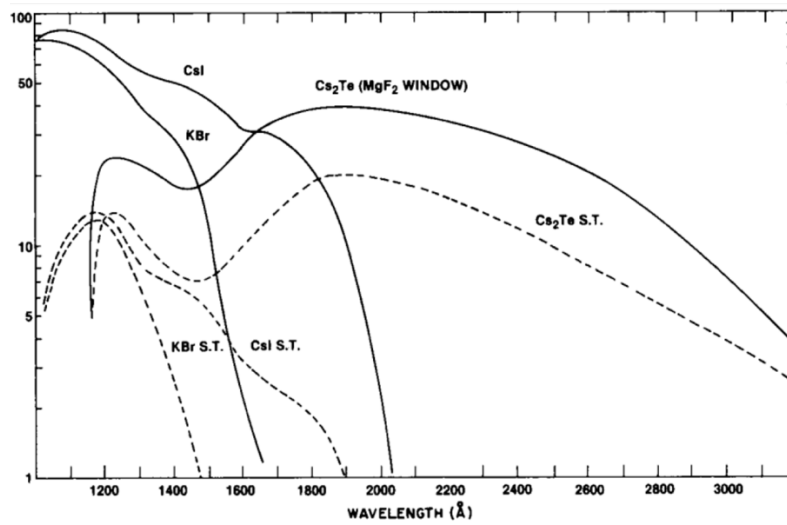


Figure 3a. Quantum efficiency (%) of various materials often used in the photocathodes of the UV detectors, both in opaque and semi-transparent (S.T.) modes of operation (Carruthers, 2000). The percent of ejected photoelectrons per impinging photons is represented in the Y-axis. Semitransparent photocathodes are used in the astronomical applications with efficiencies below 20%. This technology has evolved significantly in the last decade. Depositing the photosensitive substrate directly in the MCP micro-tubes and slight variations in the micro-tubes geometry have proven to rise the efficiency by a factor of ~2.

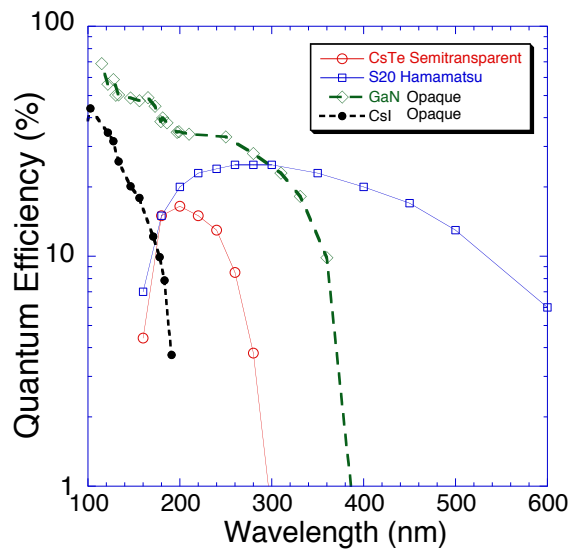


Figure 3b. Current status on the investigation of new materials to improve the quantum efficiency of the MCP substrates. In addition to the classical substrates like CsTe or CsI, new materials are coming into play such as the GaN (Sigmund et al. 2019).

#### 4. The procedure implemented by the IAU WG on UV Astronomy for band definition.

A first selection was made by the IAU WG on UV Astronomy (UVA WG) consisting in:

- Three NUV bands: NUV<sub>1</sub>(GALEX NUV blue edge to 210 nm), NUV<sub>2</sub> (210 nm -235nm), NUV<sub>3</sub>(235 nm-275 nm).
- GALEX FUV band.
- Two to three bands (to be defined) to cover the 90-140nm spectral range.

Following this, community feedback was solicited. A questionnaire was distributed through the International Astronomical Union network, via the website pages belonging to the UVA-WG. Also, a general mailing to the registered members of the global Network for Ultraviolet Astronomy (gnuva.net) was issued. The feedback from this poll is summarized in Appendix C.

The results from the poll, together with the deliberations of the UVA-WG have been used to define the first tentative list of filters (see Table 2).

Table 2: UV photometric bands proposed as standards

Band ID	Spectral Range	Objective	Comments on implementation
UV1	90-110 nm	FUSE window	
UV2	120-140 nm	Far UV avoiding geocoronal Ly-alpha	[CsI photocathode + F125LP (CaF <sub>2</sub> )] – [ CsI photocathode +F140LP (BaF <sub>2</sub> ) ]
UV3	140-180 nm	GALEX FUV	As in GALEX
UV4	180-210 nm	Continuum shortward of the UV bump	
UV5	210-230 nm	UV bump	
UV6	230-280 nm	Near UV continuum, Fe bands	F250W (ACS/HRC)
UV7	280-350 nm	Ozone cut-off window	F330W(ACS/HRC)

#### 5. The photometric system.

To visualize the characteristics of the system, the UV<sub>1-7</sub> magnitudes have been computed for Hubble's spectrophotometric standards in the Vega system<sup>e</sup>; only 46 of them have been observed in the 115-400 nm spectral range (see Appendix C), and just 3 (including Vega) have been observed with FUSE. As shown in Appendix C, most of the sources are A-type stars or white dwarf stars. The UV bands and UV colors are plotted in Figure 4 and color-color diagrams for these 45 sources are displayed in Figure 5.

---

<sup>e</sup> Vega is included in the list of Hubble spectrophotometric standards. For the UV photometric system definition Vega's UV<sub>1-7</sub> magnitudes have been set to zero.

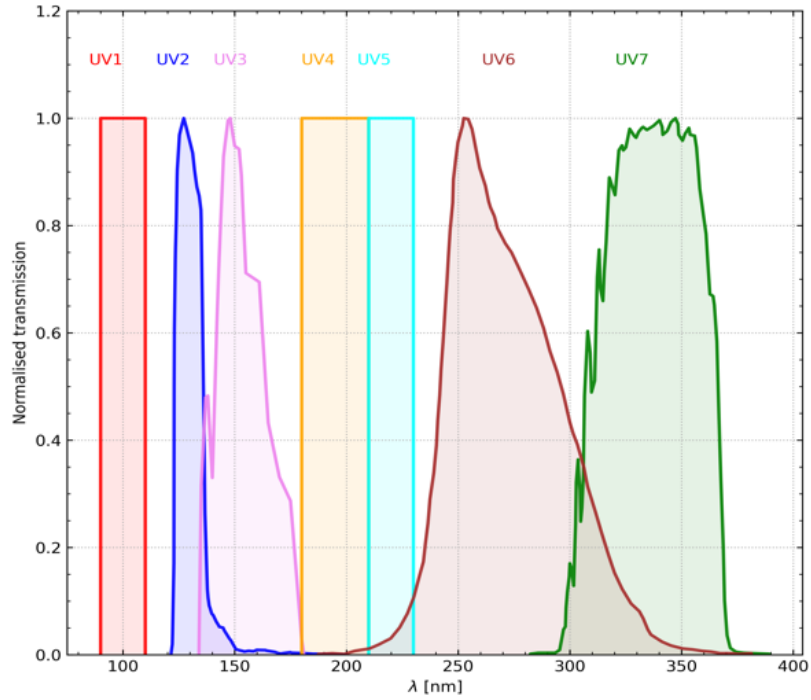


Figure 4. Tentative UV bands. Some of them, UV2, UV3, UV6 and UV7, are already implemented since they come from Hubble instruments or from GALEX. For the new bands, simple (unrealistic) boxcar functions have been used with transmittances similar to the rest of the bands.

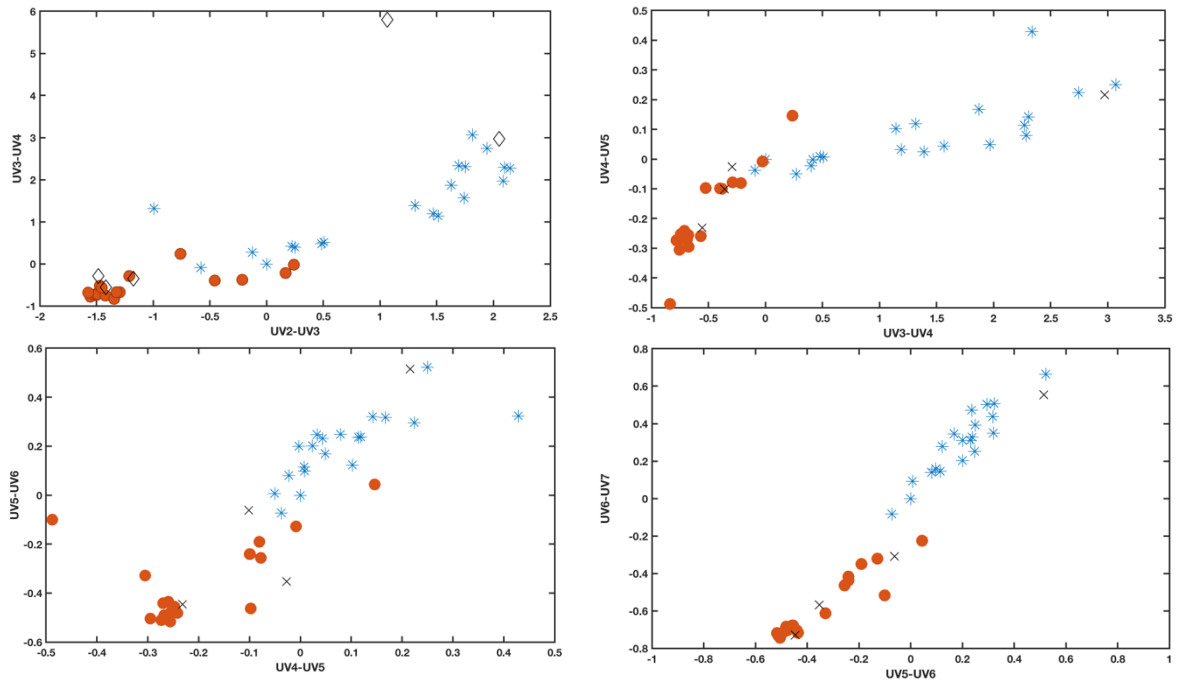


Figure 5. Color-color diagrams for the UV spectrophotometric standards (red circles: white dwarfs; asterisks: A-type stars; black crosses: other types)

The spatial distribution of these standards on the sky is represented in Figure 6.

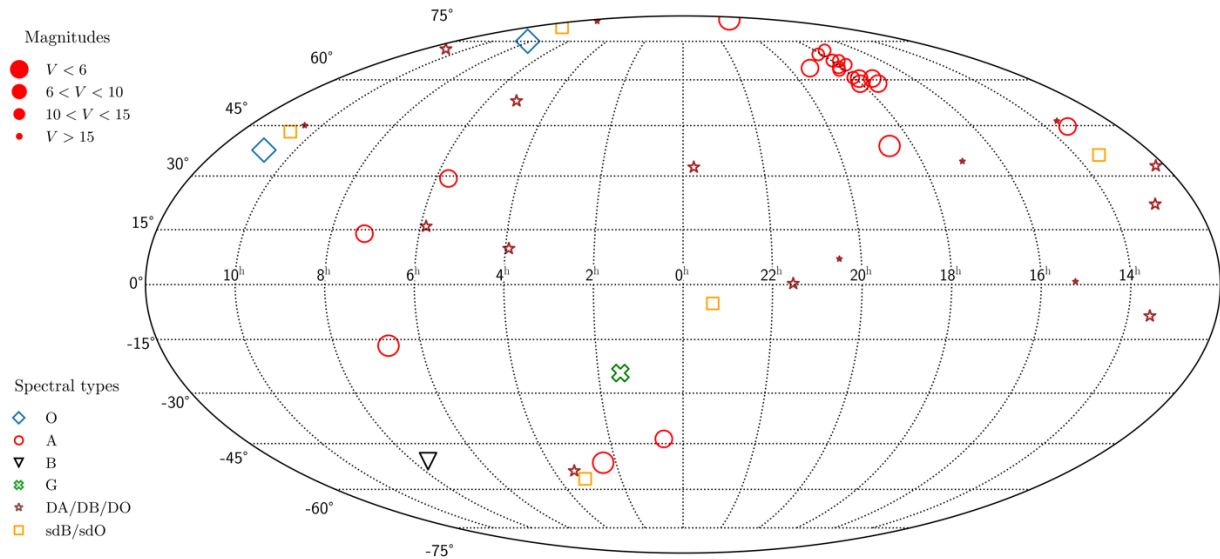


Figure 6. Distribution of UV photometric standards in the sky.

## 6. Example of implementation for minisats and cubesats

The Star-Planet Activity Research Cubesat (SPARCS) is one of the very few cubesats being currently under implementation for astronomical imaging in the ultraviolet. The key scientific objective of the mission is to monitor the high-energy radiation environment of the habitable zone exoplanets around M Dwarfs. Earth-like planets are easier to find around low mass stars and the scientific community is investing significant efforts to detect them. However, unlike solar-type stars, M dwarfs stay active with high emission levels and frequent flares throughout their lives (Shkolnik and Barman 2014). The effects of sustained high levels of stellar activity on planetary atmospheres have not been studied since UV flare rates and energies across time are not well-known. Yet, we can expect that the increased UV emission and associated particle flux will have dramatic effects on a planet's atmosphere (e.g., Segura et al. 2010; Luger and Barnes 2015).

The UV emission probed by SPARCS can photodissociate important diagnostic molecules in a planetary atmosphere, such as water ( $H_2O$ ), ozone ( $O_3$ ), sulfur dioxide ( $SO_2$ , a signature of volcanic activity), and ammonia ( $NH_3$ ), an important source of the nitrogen required to build amino acids (Fig. 7, right panel).

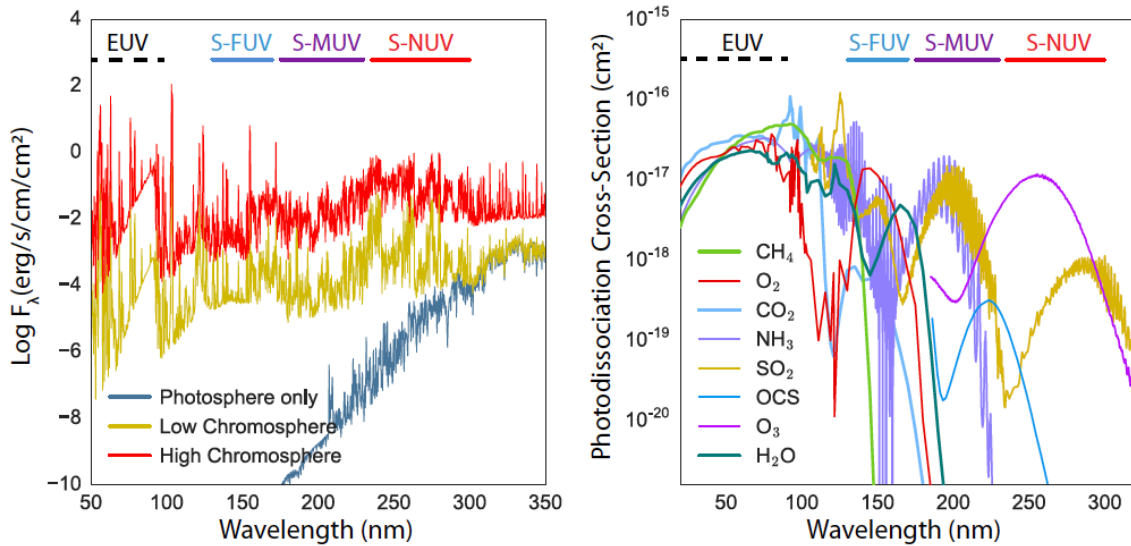


Figure 7. SPARCS UV filters probe key spectral regions important for both M dwarf non-thermal emission and exoplanet atmospheric molecules. Left: UV emission from M dwarfs atmosphere. Right: Cross section to photodissociation by UV radiation of relevant atmospheric molecules. The spectral coverage of the SPARCS UV filters (S-FUV, S-MUV, S-NUV) is shown in both panels.

The transmittance of the filters (including the contribution from the detector spectral sensitivity) is shown in Figure 8. The filter S-FUV is slightly shifted with respect to UV3 (GALEX FUV) to optimize the sensitivity to the CIV and He II lines. The filter S-NUV is similar to UV6 and the S-MUV is the sum of filters UV4+UV5.

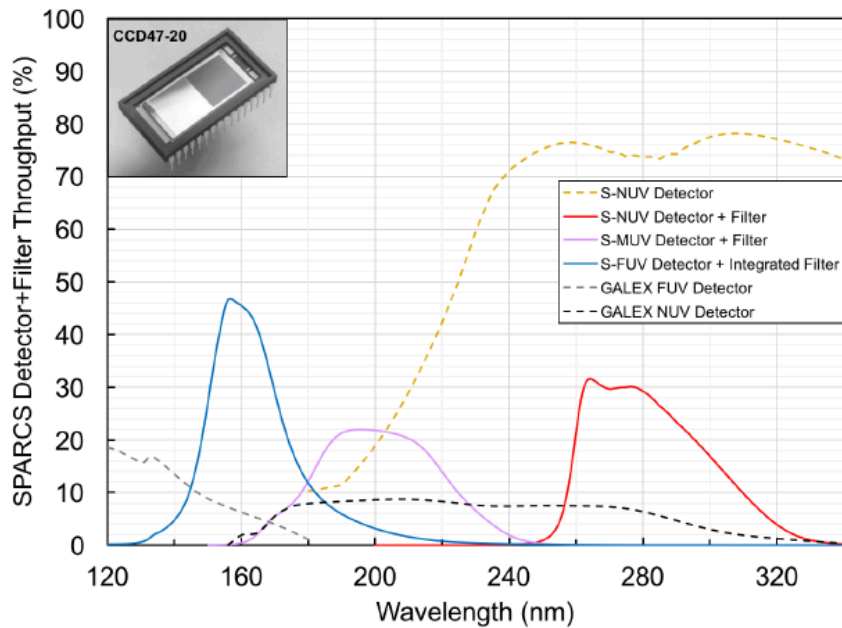


Figure 8. SPARCS throughput in the S-FUV, S-MUV and S-NUV bands.

SPARCS bands were defined for a very specific scientific purpose, still they are very close to the UV1-7 system proposed in this report. Moreover, given that the underlying spectral energy distribution of the sources is known (M-type stars), SPARCS magnitudes could easily be converted into a standard UV1-7 photometric system.

## **7. Concluding remarks.**

This report shows that defining a UV photometric system is feasible and useful. It is feasible because many missions and researchers have independently defined filters for their science that are rather similar (see Figure 1). Table 1 is based on data from medium-large missions but it will likely be applicable for small and cubesat-like missions. Providing our community with a reference framework, a common photometric system and the associated tools, it is important for the efficient and rigorous use of the large wealth of data being acquired.

The photometric system proposed in Section 5 cannot be implemented in terms of the optical description (transmittance curves) of filters. The reflectivity of the coatings and the sensitivity of the detectors vary significantly in the UV range; as shown in Figure 7, the performance of a UV instrument depends on the combined effect of all these components. As a consequence, the implementation of the system needs to be done “a posteriori” by post-processing the data from the individual missions into the standard system. The methods to define this standardization should be the core of the activity of the UV Astronomy WG after approval and dissemination of this document. The computational resources already available and the wealth of information in the astronomical archives will certainly aid in the process.

This type of activity belongs to one of IAU’s fundamental roles: to define standards of reference for information exchange. The fundamentals of the scientific method lie in the ability to test results by independent researchers and this requires the definition of a clear and accessible framework for the interpretation of the data.

Finally, we would like to emphasize that there are currently several UV missions in definition, each with a different set of filters and it would be very convenient to have a common framework for broad band photometry in all of the them.

## Bibliography

- Bohlin, R.C., et al., 1990, *ApJS*, 73, 413.
- Bohlin, R.C., 1994, *Proceedings of STScI HST Calibration Workshop*, eds. A. Koratkar & C. Leitherer, p. 49.
- Bohlin, R.C., Colina, L., & Finlay, 1995, *AJ*, 110, 1316.
- Bohlin, R.C., 1996, *AJ*, 111, 1743.
- Bohlin, R.C., Gordon, K.D., Tremblay, P.E., 2014, *PASP*, 126, 711
- Carruthers, G.R., 2000, "Ultraviolet and X-ray detectors," *Electro-Optics Handbook*.
- Hamuy et al., 1992, *PASP*, 104, 533.
- Hayes & Latham, 1975, *A. J.* 197, 593.
- Luger, R., and R. Barnes 2015. Extreme Water Loss and Abiotic O<sub>2</sub> Buildup on Planets Throughout the Habitable Zones of M Dwarfs. *Astrobiology* 15, 119–143.
- Segura, A., L. M. Walkowicz, V. Meadows, J. Kasting, and S. Hawley 2010. The Effect of a Strong Stellar Flare on the Atmospheric Chemistry of an Earth-like Planet Orbiting an M Dwarf. *Astrobiology* 10, 751–771.
- Shkolnik, E. L., and T. S. Barman 2014. HAZMAT. I. The Evolution of Far-UV and Near-UV Emission from Early M Stars. *AJ* 148, 64,14pp.
- Shugarov, A., Savanov, I., Sachkov, M. et al., 2014, *ApSS*, 354, 169.
- Siegmund, O. H., Vallergera, J., Darling, N., et al., 2019, *Proc. SPIE UV X-Ray, and Gamma-Ray Space Instrumentation for Astronomy XXI*, Vol. 11118, 111180N (9 September 2019)
- Thompson et al. , 1978, *Scientific Research Council*.
- Turnshek, D.A., Bohlin, R.C., Williamson, R., Lupie, O., Koornneef, J., & Morgan D. 1990, *AJ*, 99, 1243

## APPENDIX A

Table A.1: List of HST spectrophotometric standards.

Star name	R.A. (2000)	Declination (2000)	Sp. T.	V	B-V	Vr (km/ s)	PM (mas/yr)	
							$\mu_{\alpha}\cos\delta$	$\mu_{\delta}$
HZ43 <sup>(a)</sup>	13 16 21.853	+29 05 55.38	DA	12.91	-0.31	54	-157.96	-110.23
SDSS132811	13 28 11.498	46 30 50.94	DA	g=17.01	...		-130.86	-30.8
WD0320-539	03 22 14.820	-53 45 16.47	DA	14.9	...	57.8	6.56	-59.93
WD0947+857	09 57 54.296	85 29 40.88	DA	16.4	...		-28.13	-27.27
WD1026+453	10 29 45.295	+45 07 04.93	DA	16.13	-		-90.46	1.68
G191B2B	5 05 30.618	+52 49 51.92	DA.8	11.781	-	22.1	12.59	-93.52
WD1657+343	16 58 51.113	+34 18 53.32	DA.9	16.1	0.33		8.77	-31.23
GD153	12 57 02.322	+22 01 52.63	DA1.2	13.349	-	25.8	-38.41	-202.95
WD1057+719	11 00 34.243	+71 38 02.92	DA1.2	14.68	0.29	76	-43.64	-21.75
GD71	5 52 27.620	+15 53 13.23	DA1.5	13.032	...	23.4	76.84	-172.94
SDSS151421	15 14 21.273	+00 47 52.81	DA1.8	16.5	0.25	12	4.4	-27.04
GRW+70 5824	13 38 50.478	+70 17 07.64	DA2.4	12.6	-	26	-402.09	-24.61
HZ4	03 55 21.988	+09 47 18.13	DA3.4	14.51	0.06	46	173.27	-5.51
WD1327-083	13 30 13.637	-08 34 29.47	DA3.5	12.34	0.09	36	-1111.1	-472.38
WD2341+322	23 43 50.721	+32 32 46.73	DA3.8	12.94	0.06	-16	-215.82	-59.74
LDS749B	21 32 16.233	+00 15 14.40	DBQ4	14.674	-	-81	413.23	27.27
GJ754.1A	19 20 34.923	-07 40 00.07	DBQA 5	12.29	0.04		-61.28	-161.77
HZ21	12 13 56.264	+32 56 31.36	DO2	14.69	-		-100.88	30.13
HS2027+0651	20 29 32.506	+07 01 07.70	DO	16.9	0.33		9.24	1.53
AGK+81 266	09 21 19.177	+81 43 27.63	sdO	11.95	...		-11.26	-51.26
FEIGE110	23 19 58.400	-05 09 56.17	sdO	11.83	-		-10.68	0.31
FEIGE34	10 39 36.738	+43 06 09.21	sdO	11.14	-0.3	1	12.54	-25.41
HZ44	13 23 35.263	+36 07 59.55	sdB	11.65	-		-66.27	-4.52
SNAP-1	16 29 35.747	+52 55 53.61	sdB	15.4	0.23		-3.16	-20.8
WD0308-565	03 09 47.918	-56 23 49.41	sdB	14.07	0.2	-68	149.24	66.92
BD+17 4708 <sup>(b)</sup>	22 11 31.375	+18 05 34.16	sdF8	9.47	-0.11	-291	506.37	60.49
BD+54 1216	08 19 22.572	+54 05 09.63	sdF6	9.71	0.44	66	-34.2	-628.56
HD074000	08 40 50.804	-16 20 42.51	sdF6	9.66	0.48	206	350.82	-484.16
BD+75 325	08 10 49.490	+74 57 57.94	O5P	9.55	0.45	-50	7.17	10.3
MU COL	05 45 59.895	-32 18 23.16	O9.5V	5.15	0.33	109	2.99	-22.03
10 Lac	22 39 15.679	+39 03 00.97	O9V	4.88	-	-10	-0.32	-5.46

HD93521	10 48 23.512	+37 34 13.09	O9Vp	6.99	-	-14	0.22	1.72
LAM LEP	05 19 34.524	-13 10 36.44	B0.5IV	4.27	-	20	-3.3	-4.91
HD60753 <sup>(c)</sup>	07 33 27.319	-50 35 03.31	B3IV	6.68	-	20	-3.12	5.31
ETA UMA	13 47 32.438	+49 18 47.76	B3V	1.85	-0.1	-13	-121.17	-14.91
ksi2 Ceti	02 28 09.557	+08 27 36.22	B9III	4.28	-	12	23.71	-4.79
109 Vir	14 46 14.925	+01 53 34.38	A0III	3.73	-	-6.1	-114.03	-22.13
ALPHA LYR	18 36 56.336	+38 47 01.28	A0V	0.031	0	-21	200.94	286.23
ETA1 DOR	06 06 09.382	-66 02 22.63	A0V	5.69	-	17.6	13.66	27.82
HD116405	13 22 45.124	+44 42 53.91	A0V	8.34	-	-19	8.01	-10.29
HD180609	19 12 47.200	+64 10 37.17	A0V	9.42	0.15		-3.06	-7.79
BD+60 1753	17 24 52.277	+60 25 50.78	A1V	9.65	0.07		3.98	1.81
DELTA UMI	17 32 12.997	+86 35 11.26	A1V	4.34	0.03	-7.6	10.17	53.97
HD128998	14 38 15.222	+54 01 24.02	A1V	5.83	0	-3	17.28	-18.99
SIRIUS	06 45 08.917	-16 42 58.02	A1V	-1.46	0	-6	-546.01	-1223.1
HD101452	11 40 13.6509	-39 08 47.674	A2/3	8.2	-		<b>-34.166</b>	-20.98
2MASS J18022716+6043356	18 02 27.17	+60 43 35.7	A2V	11.98	0.02			
2MASS J17571324+6703409	17 57 13.233	+67 03 40.77	A3V	12.01	-0.1		0.41	-14.03
2MASS J18083474+6927286	18 08 34.736	+69 27 28.72	A3V	11.69	0.49		4.43	8.52
HD2811	00 31 18.490	-43 36 23.00	A3V	7.5	0.17		-6.02	-4.18
HD37725	05 41 54.370	+29 17 50.96	A3V	8.31	-		15.05	-26.93
2MASS J17325264+7104431	17 32 52.630	+71 04 43.12	A4V	12.53	0.12		0.22	-2.71
2MASS J18022716+6043356	18 05 29.275	+64 27 52.13	A4V	12.28	0.14		-1.64	10.06
HD55677	07 14 31.290	+13 51 36.79	A4V	9.41	0.06	-2	-2.66	-6.81
HD158485	17 26 04.837	+58 39 06.83	A4V	6.5	0.13	-30	-9.1	14.67
HD165459 <sup>(d)</sup>	18 02 30.741	+58 37 38.16	A4V	6.86	0.13	-19.2	-13.06	24.61
BD+02 3375	17 39 45.595	+02 24 59.61	A5	9.93	0.45	-398	-366.01	75.12
BD+26 2606	14 49 02.355	+25 42 09.14	A5	9.73	0.39	33	-5.88	-347.6
2MASS J18120957+6329423	18 12 09.567	+63 29 42.26	A5V	11.74	0.2		4.07	1.31
HD14943	02 22 54.675	-51 05 31.66	A5V	5.91	0.19	5	22.33	66.38
2MASS J17403468+6527148	17 40 34.679	+65 27 14.77	A6V	12.48	0.2		-5.72	-3.44
HD163466	17 52 25.376	+60 23 46.94	A6V	6.85	0.19	-16	-2.73	42.67
2MASS J17430448+6655015	17 43 04.486	+66 55 01.66	A8III	13.52	0.28		1.10	-2.79
HD160617	17 42 49.324	-40 19 15.51	F	8.73	0.45	100	-62.39	-393.23
BD+21 0607	04 14 35.516	+22 21 04.25	F2	9.22	0.44	340	425.99	-301.87
HD031128	04 52 09.910	-27 03 50.94	F4V	9.14	0.41	112	164.76	-26.52
BD+29 2091	10 47 23.163	+28 23 55.93	F5	10.22	0.5	83	177.5	-824.83
HD111980	12 53 15.053	-18 31 20.01	F7V	8.38	0.53	155	299.49	-796.09

C26202	03 32 32.843	-27 51 48.58	F8IV	16.64	0.26				
HD200654	21 06 34.751	-49 57 50.28	G	9.11	0.63	-45	193.94	-273.89	
SF1615+001A	16 18 14.240	+00 00 08.61	G	16.75	0.49		2.40	-10.94	
HD106252	12 13 29.510	+10 02 29.89	G0	7.36	0.64	16	22.86	-280.01	
SNAP-2	16 19 46.103	+55 34 17.86	G0-5	16.23	0.86		-2.91	-10.95	
HD209458 <sup>(e)</sup>	22 03 10.773	+18 53 03.55	G0V	7.65	0.59	-15	29.58	-17.89	
P177D	15 59 13.579	+47 36 41.91	G0V	13.49	0.6		-7.9	1.57	
HD38949	05 48 20.059	-24 27 49.85	G1V	7.8	0.57	3	-30.44	-35.42	
HD159222	17 32 00.992	+34 16 16.13	G1V	6.56	0.65	-52	-240.7	63.71	
18 Sco	16 15 37.270	-08 22 09.98	G2V	5.5	0.65	11.9	232.16	-495.37	
HD37962	05 40 51.966	-31 21 03.99	G2V	7.85	0.65	3	-59.65	-365.23	
HD205905	21 39 10.151	-27 18 23.67	G2V	6.74	0.62	-17	384.1	-83.96	
P330E	16 31 33.813	+30 08 46.40	G2V	12.92	0.64	-53	-8.99	-38.77	
16 Cyg B	19 41 51.973	+50 31 03.09	G3V	6.2	0.66	-27.7	-134.79	-162.49	
HD115169	13 15 47.388	-29 30 21.18	G3V	9.2	0.69	21.2	-110.57	-82.09	
HD167060	18 17 44.143	-61 42 31.62	G3V	8.92	0.64	15.2	88.52	-145.15	
HD185975	20 28 18.740	-87 28 19.94	G3V	8.1	0.68	-19	169.76	-56.99	
HD142331	15 54 19.788	-08 34 49.37	G5V	8.75	0.64	-70.8	-105.98	-23.73	
HD009051	01 28 46.503	-24 20 25.44	G7III	8.92	0.81	-72	53.56	-17.03	
P041C <sup>(f)</sup>	14 51 57.980	+71 43 17.39	GOV	12.16	0.68	-22	-49.32	19.58	
KF08T3	17 55 16.216	+66 10 11.61	K0.5III	13.18	1.21	-50	2.09	-6.39	
KF06T2	17 58 37.995	+66 46 52.11	K1.5III	13.8	1.3		0.62	-4.42	
BD-11 3759	14 34 16.812	-12 31 10.42	M3.5V	11.32	1.6	-1	-355.04	593.22	
HZ43B <sup>(a)</sup>	13 16 21.495	+29 05 53.07	M3Ve	14.3	...				
VB8	16 55 35.256	-08 23 40.75	M7V	16.92	1.8	15	-813.42	-870.61	
2M0559-14	05 59 19.188	-14 04 49.22	T4.5	J=13.80	...		570.2	-337.59	
2M0036+18	00 36 16.112	+18 21 10.29	L3.5	J=12.47	...	19	901.56	124.02	

(a) HZ43 and HZ3B are separated by  $\sim 3$ arcsec; (b) BD+17 4708 is variable (Bohlin & Landolt 2015); (c) No single model fits well in the sense that an unresolved cool companion would explain the problem; (d) Dust ring (Bohlin et al, 2011); (e) Transiting Planet; (f) P041C has an M companion 0.57arcsec away (Gilliland & Rajan 2011)

## APPENDIX B

The sky coverage of the UV imaging observations in Table 1 is represented graphically in ICRS coordinates in this appendix.

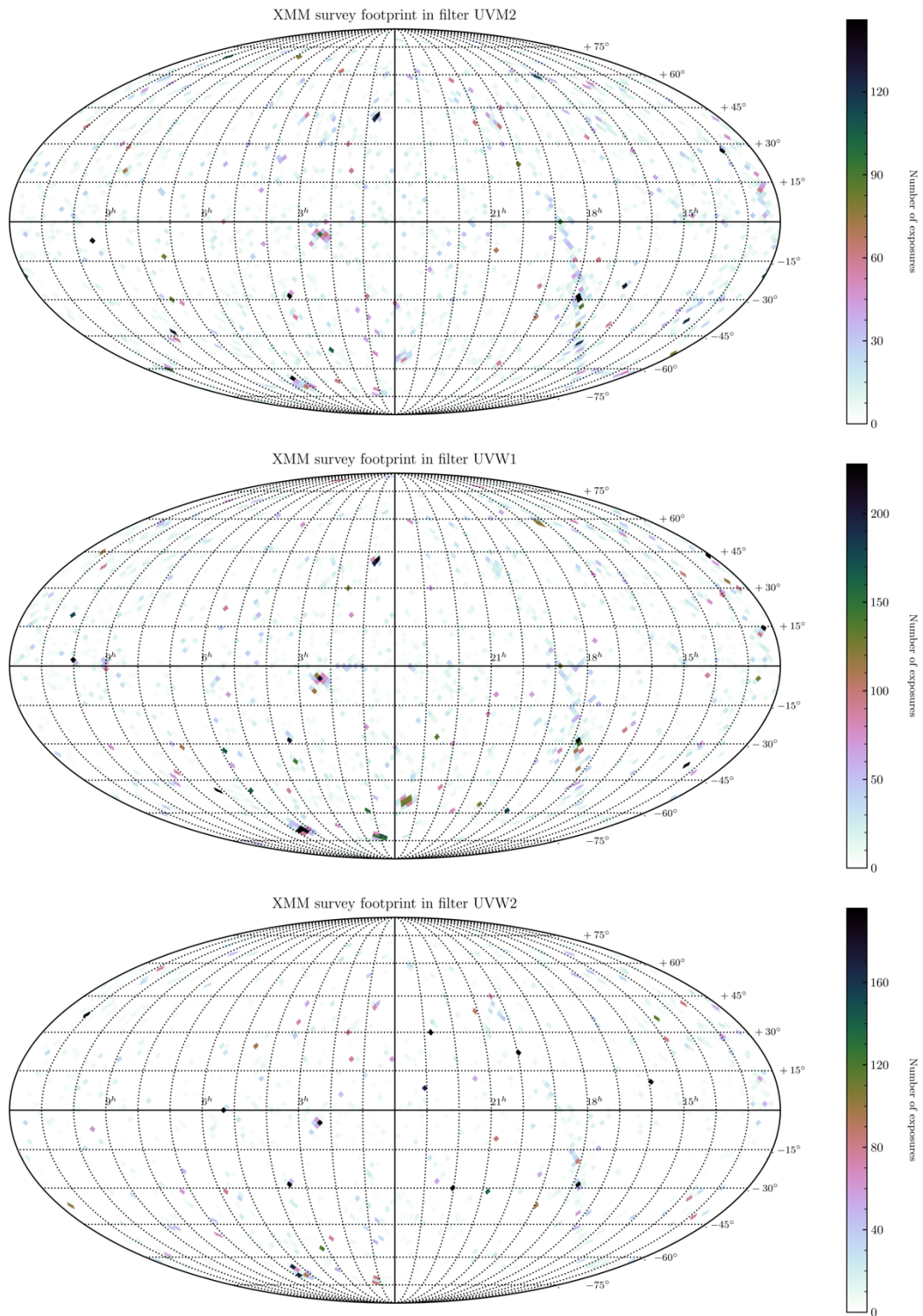


Figure B-1: Sky coverage of the observations with the XMM-Newton/OM.

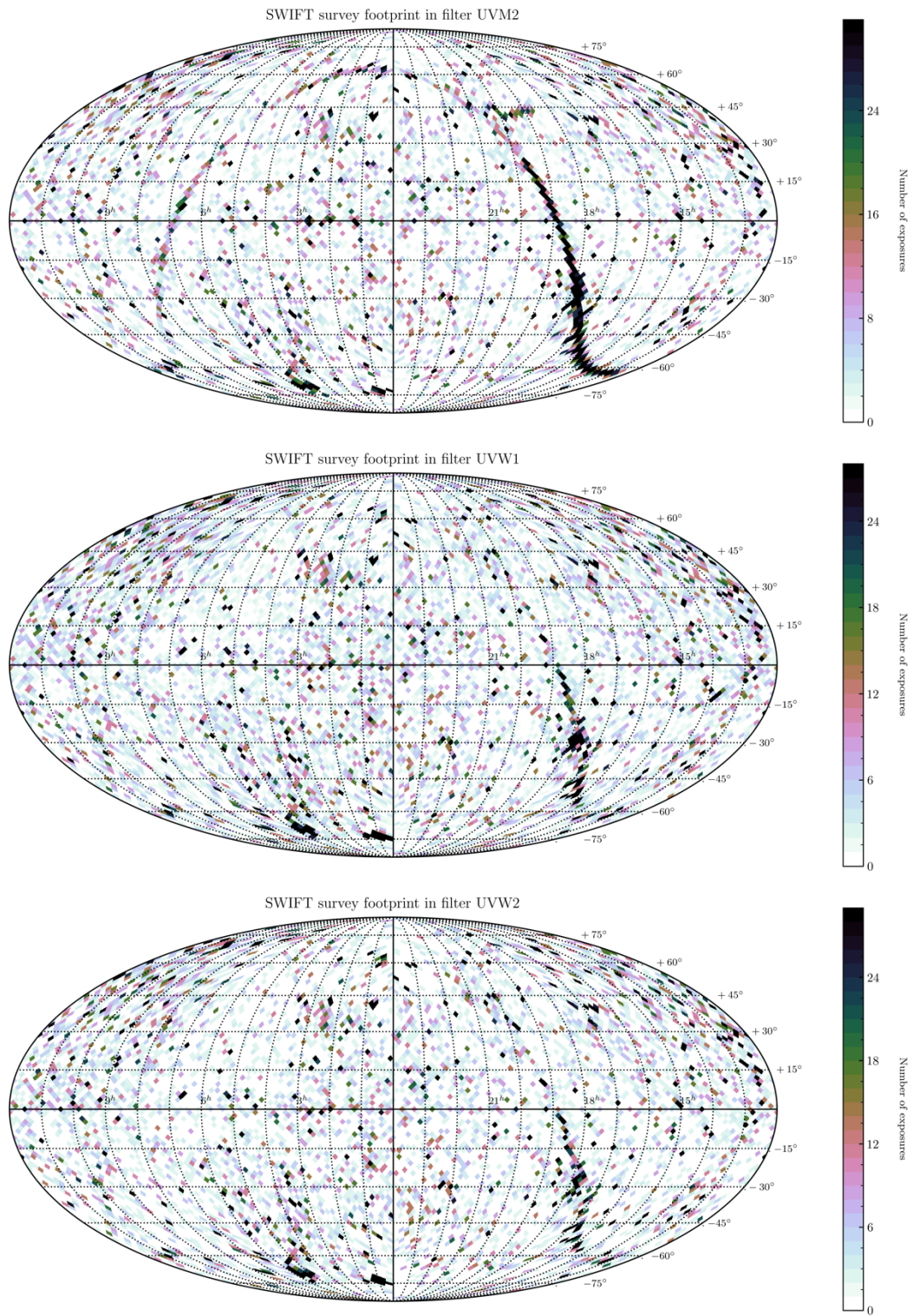


Figure B-2: Sky coverage of the observations with the SWIFT/UVOT

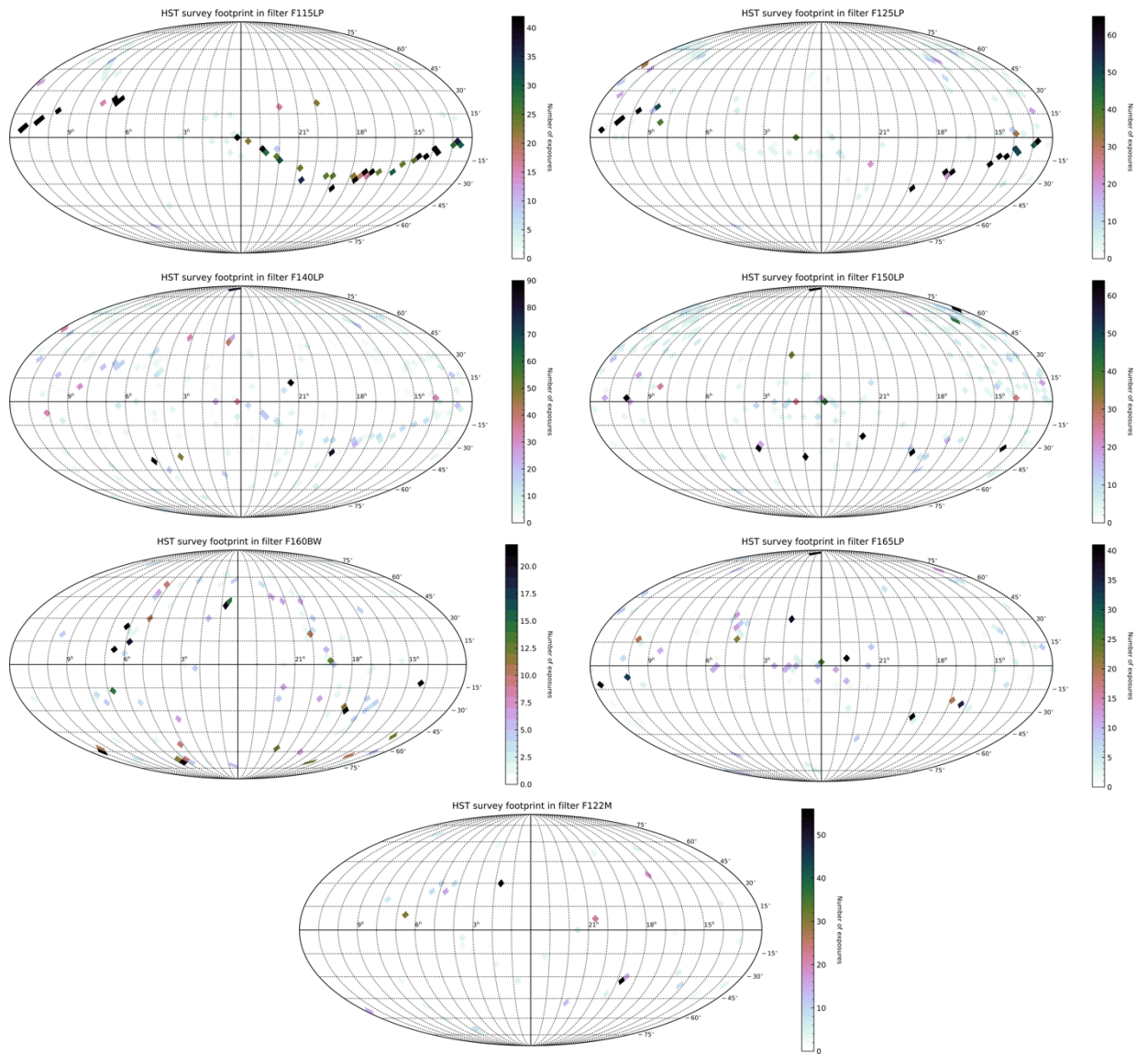


Figure B-3: Sky coverage of the observations with HST/ACS/SBC. The size of the fields has been enhanced to assist the visualization.

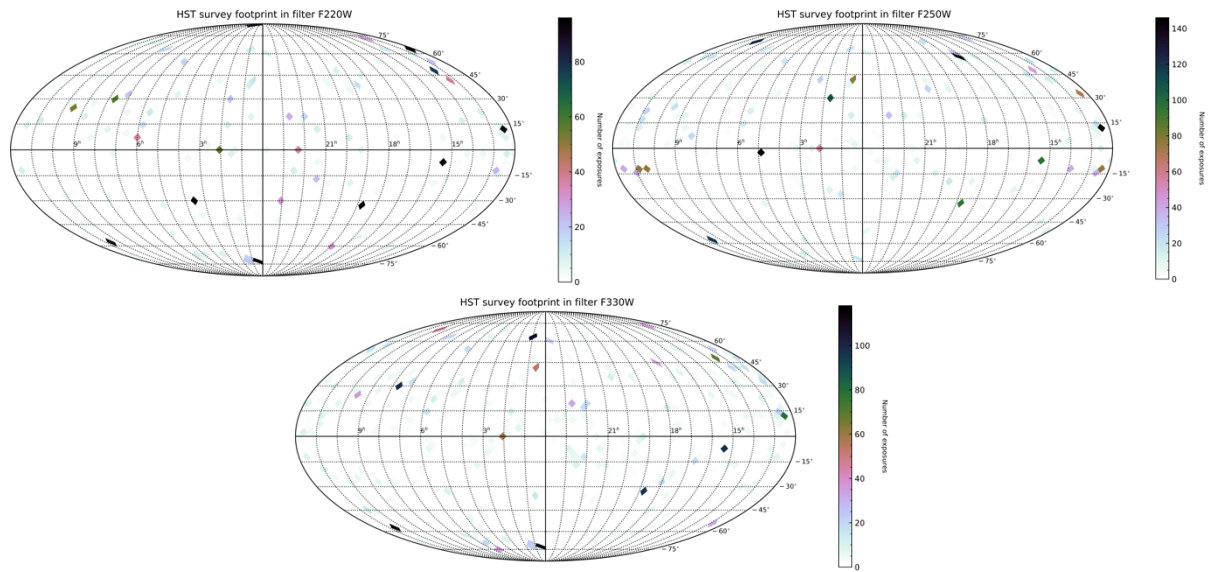


Figure B-4: Sky coverage of the observations with HST/ACS/HRC. As in Figure B-3, the size of the fields has been enhanced to assist the visualization.

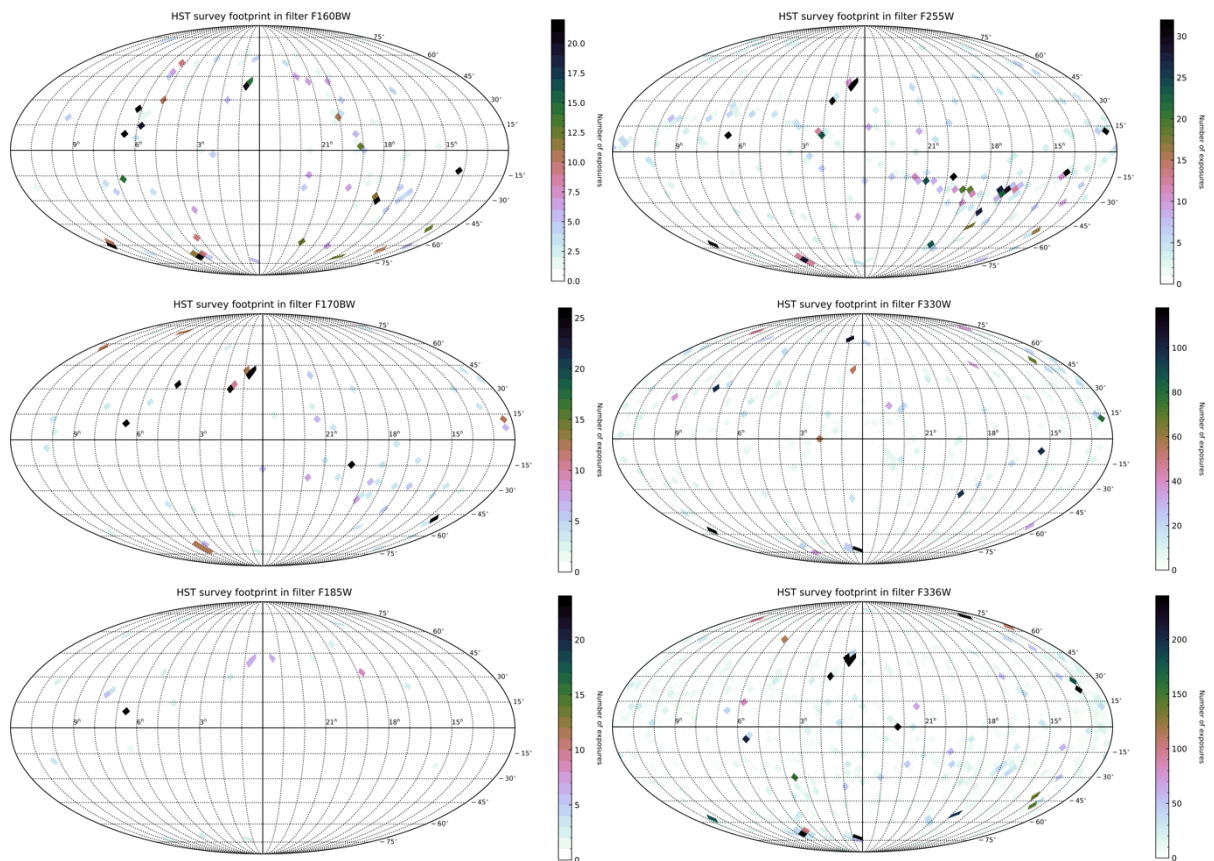


Figure B-5: Sky coverage of the observations with HST/WPC2. As in Figure B-3, the size of the fields has been enhanced to assist the visualization.

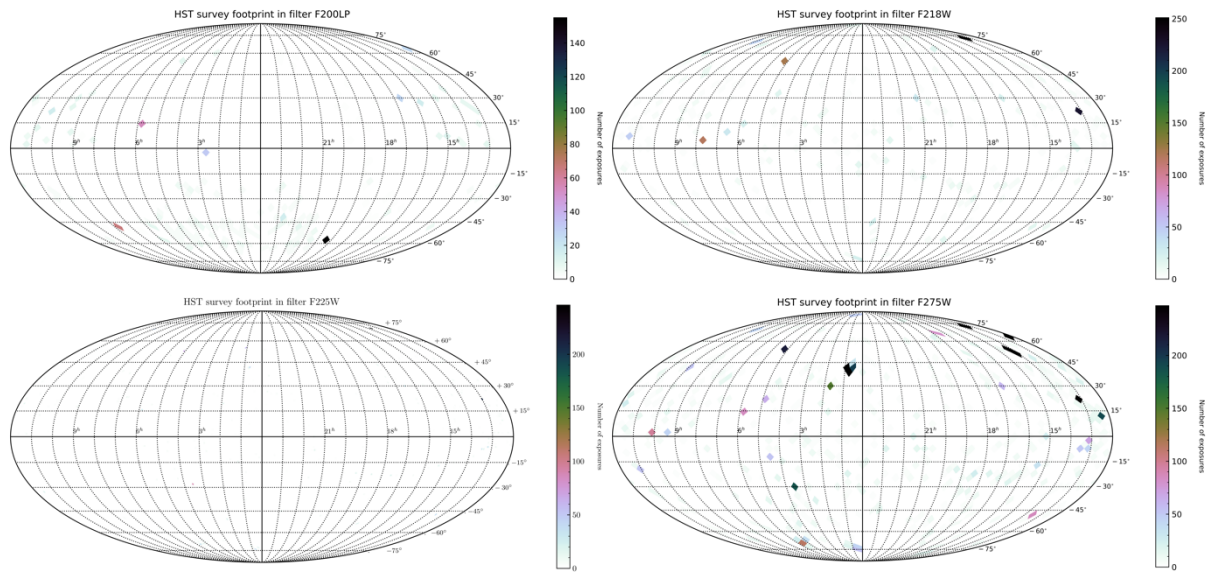


Figure B-6: Sky coverage of the observations with HST/WFC3. As in Figure B-3, the size of the fields has been enhanced to assist the visualization.

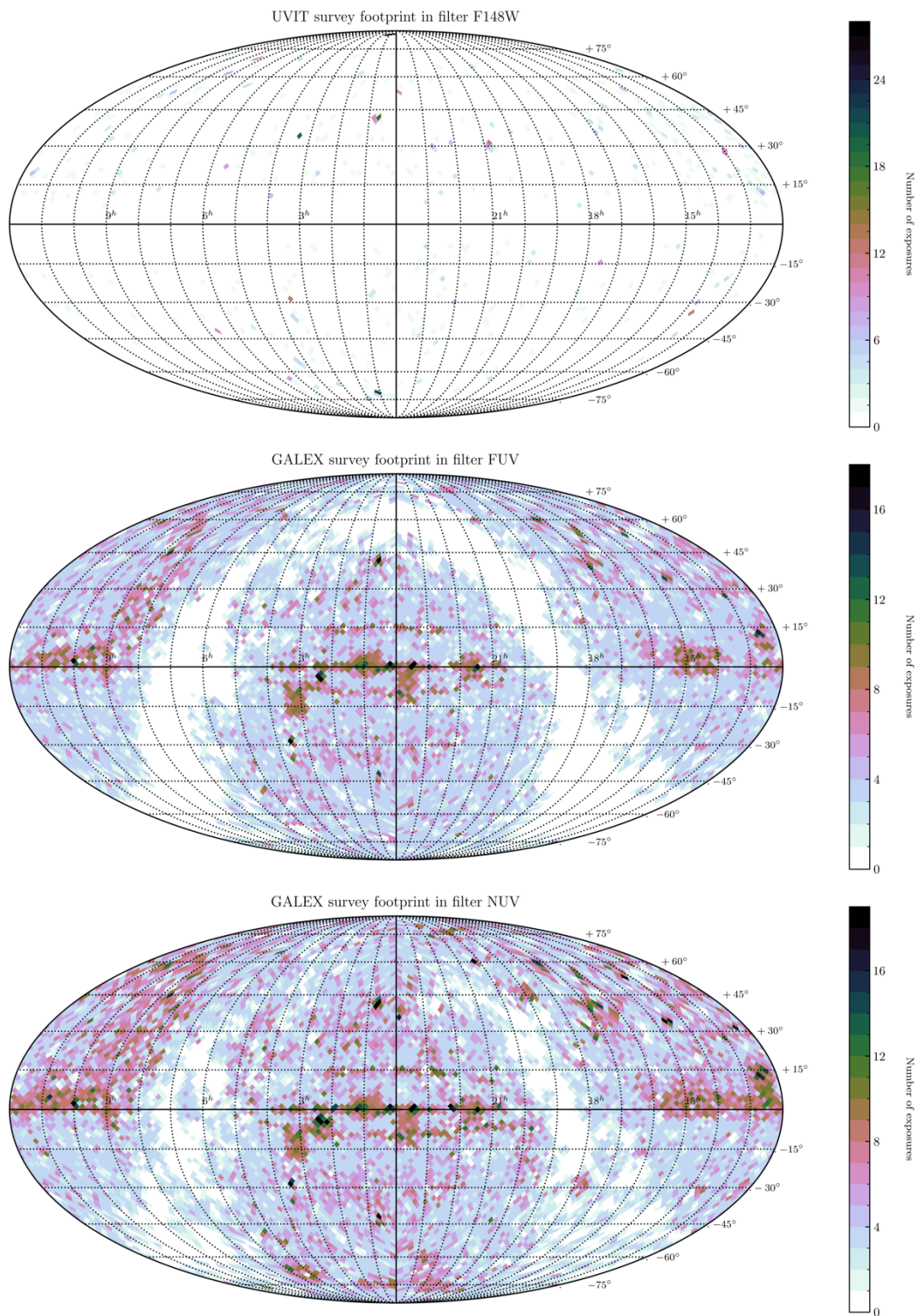


Figure B-7: Sky coverage of the observations with ASTROSAT/UVIT (top) and GALEX/FUV and GALEX/NUV. Note that for the GALEX survey only the center of the field is plotted on the graph; the actual coverage is much larger. As indicated in Table 1, the sky coverage is the same for all ASTROSAT/UVIT filters.

## APPENDIX C

In May 2019, a questionnaire was distributed to astronomers world-wide in the following terms:

The current aim of the IAU WG on UV astronomy is to define a standard photometric system for the 900-3000 Angstroms spectral range. The sample photometric system is composed by:

1. Three NUV bands: NUV1(GALEX NUV blue edge to 210 nm), NUV2 (210 nm - 235nm), NUV3(235 nm- 275 nm).
2. GALEX FUV band.
3. Two to three bands (to be defined) to cover the 90-140nm spectral range.

We expect to receive comments on the above presented photometric system or suggestions about alternative filters that could be useful for future UV science. Ideally, the proposed filters should be versatile and practical for different astrophysical studies. The deadline to send your proposals is June 7th.

The IAU WG on UV Astronomy

The responses to the Poll are summarized in figure A1 where the range covered by the new filters set proposed by the members of the community are plotted and compared with the original proposal by the UVA-WG.

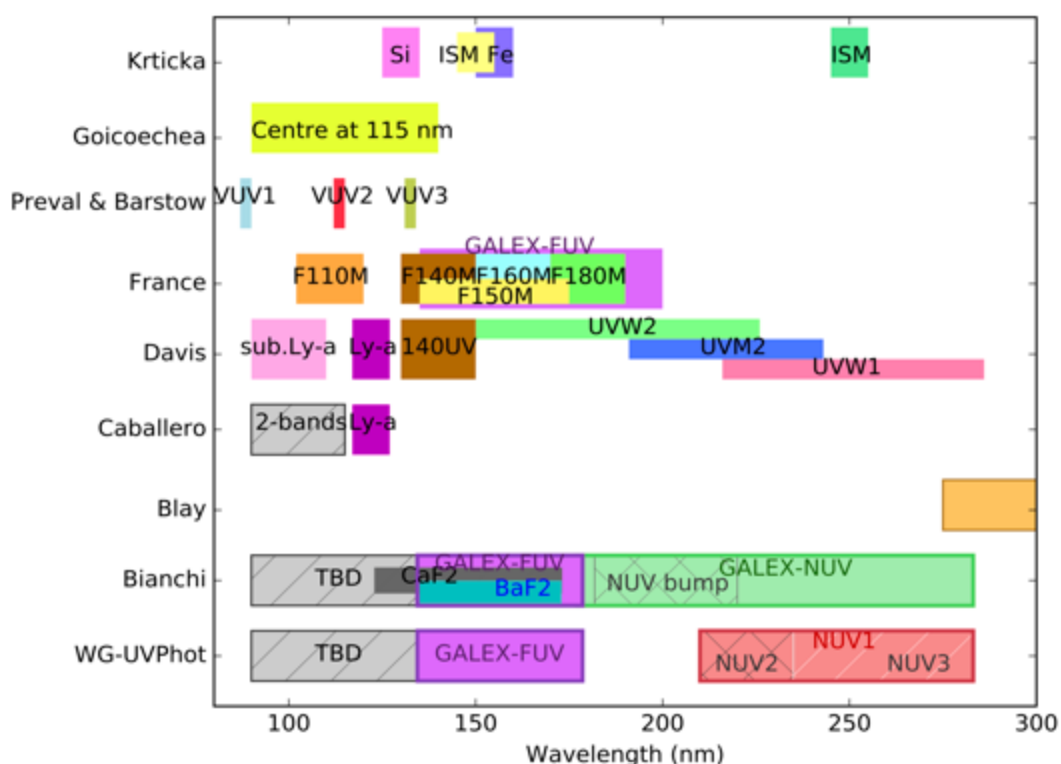


Figure B1: Summary of the bands proposed by the community in response to the questionnaire.

## APPENDIX C: List of UV Photometric Standards

Name	SpT	V	UV <sub>2</sub>	UV <sub>3</sub>	UV <sub>4</sub>	UV <sub>5</sub>	UV <sub>6</sub>	UV <sub>7</sub>	ref_spectrum
α Lyr	A0V	0.03	0.00	0.00	0.00	0.00	0.00	0.00	alpha_lyr_stis_008.fits
HD 116405	A0V	8.34	7.09	7.67	7.77	7.80	7.88	7.96	hd116405_stis_004.fits
HD 180609	A0V	9.42	12.83	11.36	10.17	10.14	9.89	9.64	hd180609_stis_004.fits
BD 60d1753	A1V	9.65	10.54	10.29	9.89	9.91	9.83	9.69	bd60d1753_stiswfc_001.fits
δ Umi	A1V	4.34	5.63	5.15	4.67	4.66	4.56	4.40	delumi_mod_001.fits
Sirius	A1V	-1.46	-1.40	-1.28	-1.55	-1.50	-1.51	-1.60	sirius_stis_002.fits
2MASS J18022716+6043356	A2V	11.98	13.37	12.87	12.36	12.35	12.23	12.09	1802271_stiswfcnic_001.fits
2MASS J17571324+6703409	A3V	12.01	18.51	16.70	13.63	13.38	12.86	12.19	1757132_stiswfc_001.fits
2MASS J18083474+6927286	A3V	11.69	17.21	15.46	13.15	13.01	12.69	12.34	1808347_stiswfc_001.fits
HD 2811	A3V	7.5	12.28	10.65	8.78	8.61	8.29	7.85	hd2811_stis_001.fits
HD 37725	A3V	8.31	13.62	11.52	9.24	9.16	8.91	8.52	hd37725_stiswfc_001.fits
2MASS J17325264+7104431	A4V	12.53	15.86	14.35	13.20	13.10	12.98	12.70	1732526_stisnic_004.fits
2MASS J18052927+6427520	A4V	12.28	16.40	14.66	13.10	13.05	12.82	12.51	1805292_stisnic_004.fits
HD 158485	A4V	6.5	9.91	8.60	7.21	7.19	6.99	6.68	hd158485_stis_004.fits
HD 165459	A4V	6.86	11.63	9.54	7.57	7.53	7.36	7.01	hd165459_stisnic_004.fits
HD 55677	A4V	9.41	10.70	10.48	10.06	10.06	9.86	9.66	hd55677_stis_001.fits
2MASS J18120957+6329423	A5V	11.74	17.38	15.69	13.35	12.92	12.60	12.09	1812095_stisnic_004.fits
HD 14943	A5V	5.91	11.88	9.93	7.19	6.96	6.67	6.17	hd14943_stis_004.fits
2MASS J17403468+6527148	A6V	12.48	13.72	14.71	13.40	13.28	13.04	12.71	1740346_stisnic_003.fits
HD 163466	A6V	6.85	12.41	10.27	8.00	7.88	7.65	7.17	hd163466_stis_004.fits
2MASS J17430448+6655015	A8III	13.52	20.16	18.12	15.14	14.93	14.41	13.86	1743045_stisnic_004.fits
HD 60753	B3IV	6.68	3.67	4.84	5.19	5.30	5.36	5.67	hd60753_stis_003.fits
WD 1326+467	DA	g=17.01	15.53	15.36	15.57	15.66	15.85	16.20	sdss132811_stis_001.fits
WD 0320_539	DA	14.9	9.47	10.95	11.66	11.92	12.37	13.05	wd0320_539_stis_004.fits
WD 0947_857	DA	16.4	10.12	11.61	12.33	12.59	13.07	13.76	wd0947_857_stis_004.fits
WD 1026_453	DA	16.13	10.59	12.08	12.79	13.03	13.51	14.20	wd1026_453_stis_004.fits
WD 0501+527	DA.8	11.69	5.84	7.40	8.18	8.45	8.96	9.69	g191b2b_fos_003.fits
WD 1657_343	DA.9	16.1	10.71	12.23	12.96	13.22	13.71	14.43	wd1657_343_stiswfcnic_001.fits
GD153	DA1.2	13.35	7.68	9.20	9.94	10.19	10.67	11.37	gd153_fos_003.fits
WD 1057_719	DA1.2	14.68	9.07	10.57	11.30	11.56	12.05	12.75	wd1057_719_stisnic_006.fits
GD71	DA1.5	13.032	7.54	9.03	9.75	10.00	10.46	11.13	gd71_fos_003.fits
SDSS 151421	DA1.8	16.5	10.77	12.19	12.95	13.25	13.58	14.19	sdssj151421_stis_001.fits
HZ4	DA3.4	14.51	12.12	12.34	12.72	12.82	13.06	13.50	hz4_stis_005.fits
WD 1327_083	DA3.5	12.34	9.70	10.16	10.56	10.66	10.90	11.31	wd1327_083_stiswfc_001.fits
WD 2341_322	DA3.8	12.94	11.81	11.57	11.60	11.61	11.73	12.06	wd2341_322_stiswfc_001.fits
LDS 749b	DBQ4	14.67	12.72	13.48	13.24	13.10	13.05	13.28	lds749b_stisnic_006.fits
HS 2027	DO	16.9	11.42	12.77	13.61	14.09	14.19	14.71	hs2027_stis_004.fits
HZ 21	DO2	14.69	8.90	10.48	11.16	11.43	11.87	12.58	hz21_stis_004.fits
HD 9051	G7III	8.92	23.59	22.53	16.73	14.13	11.57	10.00	hd009051_mod_001.fits
BD 75d325	O5p	9.55	4.05	5.47	6.02	6.25	6.70	7.43	bd_75d325_stis_004.fits
HD 93521	O9Vp	6.99	2.44	3.92	4.21	4.24	4.59	5.16	hd93521_stis_004.fits
HZ 44	sdB	11.65	6.42	7.89	8.41	8.51	8.98	9.66	hz44_fos_003.fits
WD 0308_565	sdB	14.07	10.23	11.44	11.73	11.80	12.06	12.52	wd0308_565_stis_004.fits
AGK 81d266	sdO	11.95	6.30	7.60	8.27	8.57	9.07	9.82	agk_81d266_stisnic_006.fits
Feige 110	sdO	11.83	6.38	7.83	8.40	8.66	9.09	9.81	feige110_stisnic_006.fits
Feige 34	sdO	11.14	5.55	6.87	7.55	7.80	8.32	9.04	feige34_005.fits